On the Relationship Between PRI Staggering and Sparse Arrays

Rachel J. Chang, Daniel B. Herr, Jonathan W. Owen, Patrick M. McCormick, Shannon D. Blunt, James M. Stiles
Radar Systems Lab (RSL), University of Kansas, Lawrence, KS

***Abstract*—It is well known that pulse repetition interval (PRI) staggering can expand the unambiguous Doppler domain, though doing so likewise increases Doppler sidelobes unless the staggering sequence is carefully constructed. However, there are also diversity benefits from generating random stagger sequences on-the-fly. Within the context of arbitrary stagger sequence generation, we consider the intuitive interrelation to sparse array design in the spatial domain. In so doing, the spatial co-array concept is examined for PRI staggering, along with the effect of redundancy on Doppler sidelobe levels. The physically meaningful boundaries for each domain and associated co-array attributes are observed to provide general guidelines for random PRI staggering.**

Keywords— PRI staggering, sparse array, co-array

I. Introduction

In pulse-Doppler radar, pulses are typically transmitted according to a uniform pulse repetition interval (PRI), thereby realizing a uniform sampling of slow-time (Doppler) phase that in turn aliases any Doppler exceeding half the pulse repetition frequency (PRF) [1]. In short, the unambiguous Doppler limit is $\pm\,\mathrm{PRF}/2$, where PRF is the inverse of PRI. However introducing non-uniform (i.e. staggering) PRI has the effect of expanding unambiguous Doppler in a manner that decouples (somewhat) the trade-off between unambiguous range and Doppler [2,3].

For pulse indices $m = 1, 2, \ldots, M$, denote the mth pulse repetition interval as PRI_m, which has corresponding $\mathrm{PRF}_m = 1/\mathrm{PRI}_m$. The maximum unambiguous Doppler when using staggering is thus known to be the least common multiple (LCM) of the set $\{\mathrm{PRF}_1, \mathrm{PRF}_2, \cdots, \mathrm{PRF}_M\}$ [1,2]. Proper selection of stagger interval sequences can significantly increase the unambiguous Doppler domain.

The Doppler response for random PRI staggering [4-9] still exhibits effectively the same mainlobe shape as the uniform PRI case, assuming fixed coherent processing interval (CPI) or dwell time. The sidelobes, however, become random as well, tending toward a raised and flattened response in the expectation as energy from the repeated mainlobes is smeared across Doppler [4,10]. From a detection vs. false alarm standpoint, it is preferable for a given staggered sequence instantiation to realize a flatter response (i.e. not just in the expectation). Consequently, it is prudent to consider useful attributes of pseudo-random PRI sequences, especially if on-the-fly generation is necessary.

Turning our attention to the lateral problem of sparse array design, the goal is to place array elements such that the spatial sidelobes are flattened. Clearly, there is an analogous relationship between determining the proper placement of both pulses (in time) and antenna elements to realize flattened Doppler and spatial sidelobes, respectively. This connection implies that the co-array concept employed in the latter should be applicable in the former. The relationship is explored in order to provide insight for randomly staggered PRI sequence generation. Notably, there are some "boundary effects" that lead to practical distinctions between the two domains. Moreover, the presumptive desire for *minimally redundant arrays* may not precisely translate to the PRI staggering problem, in which a small degree of redundancy (in the co-array sense) appears to yield a more preferable response.

II. The Sparse Array / Staggered PRI Analogy

There is a well-known structural similarity between the mathematical models for antenna arrays (in phase angle form) and a CPI of pulses. Indeed, the associated spatial and temporal steering vectors (generally uniform) form the basis for space-time adaptive processing (STAP) [11].

The non-uniform sampling of slow-time realized by PRI staggering uncovers Doppler attributes that are masked (aliased) by redundancy in the uniform PRI case, thereby extending unambiguous Doppler. Similarly, a non-uniform sparse array mitigates grating lobes that would otherwise occur in the spatial beampattern [12]. Of course, there is a key difference in the *purpose* of non-uniformity in each case. For staggering, the overall dwell time can be kept fixed, with non-uniform PRIs then yielding an expansion of the Doppler response. In contrast, sparse positioning allows for expansion of an antenna aperture for a fixed number of elements (hence finer spatial resolution) while mitigating the grating lobes that would otherwise arise from "under-sampling" a uniform array of the same size.

Another distinction involves the delineation of boundaries in the two domains. For a linear antenna array (uniform or non-uniform) the physical observation angle spans ±90°, noting the possibility of front/back ambiguity depending on the particular element patterns. If adjacent element spacing is less than a half-wavelength ($\lambda/2$) it is possible to exceed this *real-space* limit, beyond which lies the *imaginary-space* or *invisible-space* [13]. In practice it is preferred to avoid this regime due to the distinct potential for transmitter damage, though this concern only tends to arise for wideband applications (via fractional bandwidth perspective).

While the spatial domain element spacing is hard-limited by electromagnetic constraints, the Doppler frequency is soft-

This work was supported by the Office of Naval Research under Contract #N00014-20-C-1006. DISTRIBUTION STATEMENT A. Approved for Public Release.

limited by radial velocity between the platform and an illuminated mover. In short, the "stop-and-hop" phase progression model becomes less accurate at high scatterer velocities, thereby incurring mismatch loss. However, given that appropriate forms of receive compensation can be applied as necessary (e.g. a Doppler-tuned filter bank), and the true upper limit is the speed of light, we can effectively ignore this limit for Doppler.

Despite these domain-specific differences, the mathematical tools used for analysis and design are largely interchangeable. This similarity was explored to a degree in [14], where a sparse array design technique called Marginal Fisher's Information (MFI) [15] was used to optimize sub-Nyquist sampling based on a discretized grid. The analogy of coprime antenna arrays was likewise used in [16] to construct distinct PRI staggering sequences for subsequent combination.

Consequently, consider the useful construct for sparse array design known as the co-array concept, which is akin to performing a spatial version of autocorrelation along the axis collinear to the array and based on the locations of the particular elements. For instance, a uniform linear array (ULA) with half-wavelength element spacing exhibits a co-array comprised of impulses separated by $\lambda/2$ and having a triangular envelope. Specifically, M elements realize a weighting of M in the co-array center that linearly tapers to unity at a spatial offset of $\pm(M-1)(\lambda/2)$ and zero thereafter. Moreover, the Fourier transform of the co-array is the *spatial power spectrum* that describes the mainlobe/sidelobe response of the array (a $|\mathrm{sinc}(\cdot)|^2$ response for the ULA). It is also from the co-array that the notion of *minimum redundancy* for sparse arrays first arose (see [17]). The following considers the role of the co-array and the impact of redundancy in the context of PRI staggering.

III. PRI Staggering Co-array and Redundancy

It is common [4-10] to model staggered PRI sequences as the accumulation of sequential time intervals like that illustrated in Fig. 1. We can therefore represent this arrangement as a staggered impulse train, with each impulse denoting the start of a given pulse. Consequently, these impulses can be viewed as *locations* in a temporal aperture analogous to the element locations along a linear antenna array.

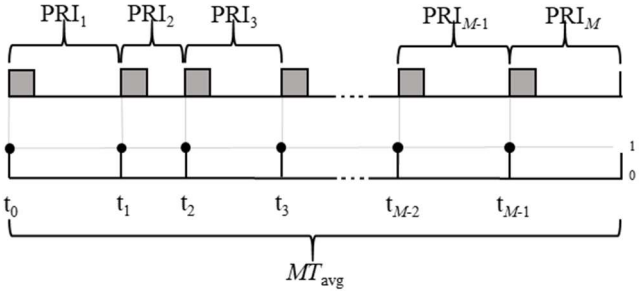

Fig. 1. Denoting the staggered pulses as an impulse train

While the impulse locations lie on a continuum in time, it is useful to impose discretization for evaluation purposes. Let "location vector" $\mathbf{w}$ therefore denote a $MK \times 1$ vector comprised of (nearly all) zeros and (a few) ones, where K is a "granularity factor" that establishes the possible stagger spacing. For a specific implementation, K is proportional to (mean PRI extent) × (bandwidth) since it depends on the number of range cells in the listen interval. Here K is arbitrarily selected for convenient comparison of different stagger structures from which to draw inferences about behavior.

The co-array (also discretized) can then be readily determined for a given location vector as [12]

$$c(\ell) = \sum_n w(n)\, w(n-\ell)\,, \tag{1}$$

which is easily recognized as an autocorrelation. The Doppler power spectrum is then the Fourier transform (FT) of (1), noting that the granularity factor K also expands the evaluated frequency domain representation by K relative to the nominal Doppler response interval of $\pm$ PRF/2 for the uniform case (depicting a repeated response for uniform PRIs). Further, while direct FT of a given staggered PRI sequence requires use of a nonuniform version [18], as does any more sophisticated Doppler processing (e.g. [19]), determining the Doppler power spectrum from (1) needs only a standard FT (along with zero-padding to aid visualization).

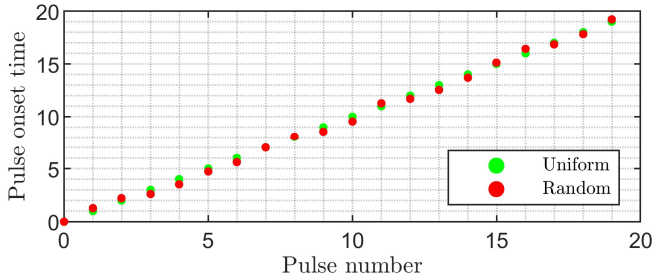

Fig. 2. Pulse onset times for uniform and random cases with 20 pulses

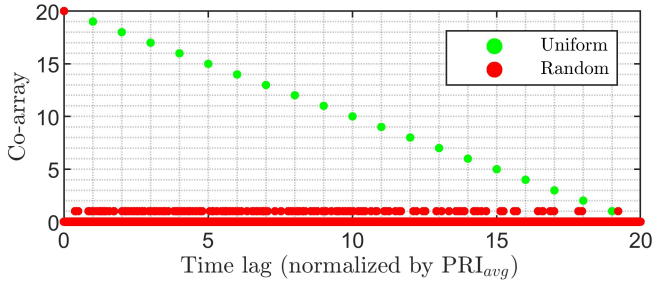

Fig. 3. Co-arrays for uniform and random cases with 20 pulses

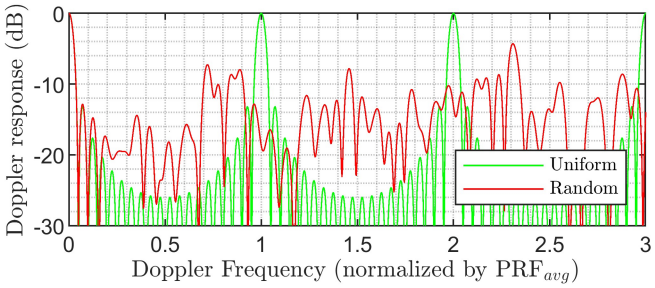

Fig. 4. Doppler responses for uniform and random cases with 20 pulses

Figs. 2-4 illustrate a comparison between uniform (green) and randomly staggered (red) PRI cases for $M = 20$ pulses and setting $K = 5000$ (i.e. very fine granularity). Fig. 2 shows the onset times for each pulse while Fig. 3 depicts the ensuing co-array for each sequence (one sided since symmetric), where the

uniform PRI case realizes the expected triangle envelope and the random instantiation naturally achieves a minimally redundant arrangement, a consequence of the fine granularity. The FT of each co-array is then shown in Fig. 4, with the usual repeated Doppler mainlobe at multiples of the uniform PRF and a somewhat flattened Doppler response for random PRIs.

While the notion of minimum redundancy in the co-array is known to provide flattened sidelobes for the spatial application, a slightly different behavior is observed for the staggering co-array due to the spatial vs. Doppler intervals being considered (i.e. their bounds are quite different). Figs. 5-7 provide a similar comparison as the previous, albeit with the inclusion of a case in which the sidelobes over the predetermined Doppler interval of $\pm$ 1.5 PRF_{avg} have been minimized via the approach in [20], where PRF_{avg} is the average PRF (i.e. same as the uniform case). This demarcation is denoted by the dashed black line in Fig. 7.

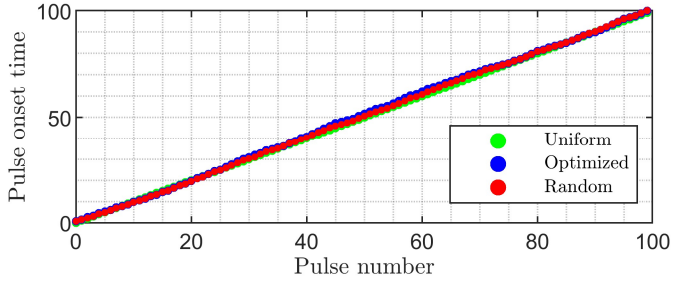

Fig. 5. Pulse onset times for uniform, random, and sidelobe-optimized PRI sequences with 100 pulses

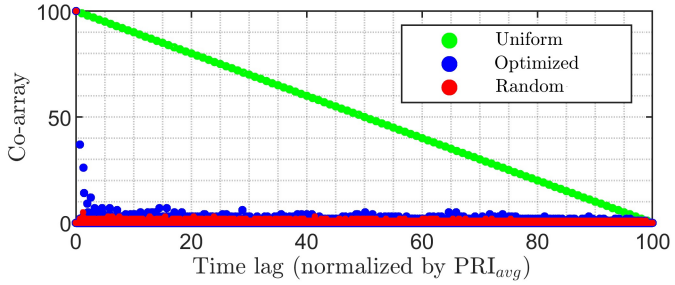

Fig. 6. Co-array for uniform, random, and sidelobe-optimized PRI sequences with 100 pulses

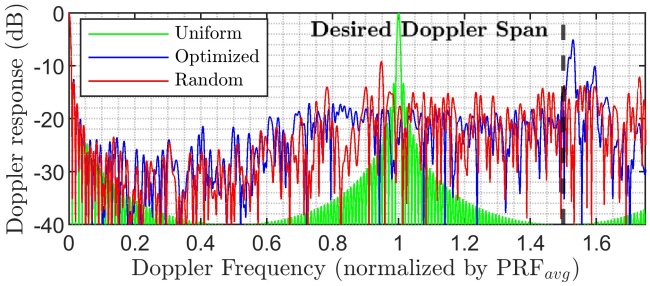

Fig. 7. Doppler response for uniform, random, and sidelobe-optimized PRI sequences with 100 pulses

The important take-away in this context is that while completely random staggering (red) does indeed provide a nearly perfect minimally redundant co-array, which in turn corresponds to somewhat flatter sidelobes, that result has no boundary in terms of a Doppler interval of interest. Therefore, we can expect to obtain an even lower/flatter sidelobe pedestal when optimizing in a manner that limits the span of the desired interval, thereby pushing higher sidelobes outside the prescribed boundary. With that said, it is interesting and potentially useful to ascertain general attributes of good random stagger sequences by considering this notion of limiting Doppler span. In so doing, it may be possible to instantiate new stagger sequences without optimization that yield a sufficiently flat response, thereby avoiding the ensuing computational cost.

For instance, another consequence of bounding the Doppler interval of interest when optimizing a stagger sequence is the close-in redundancy observed for the co-array in Fig. 6. In other words, some degree of redundancy may actually be useful.

To further illustrate the impact of co-array redundancy, 10^5 Monte Carlo trials of random PRI perturbation were performed for two different criteria. Specifically, starting with a CPI of $M = 100$ pulses having uniform PRI, each trial imposed a set of $M - 1$ independent random perturbations according to either a granularity of $K = 5$ or $K = 50$, such that the latter exhibits a 10× finer partitioning, though the actual amount of allowed stagger offset (in time) is the same for both. Consequently, we expect the former (coarser granularity) to possess higher redundancy.

Fig. 8 shows histograms for the peak Doppler sidelobe determined over the same unambiguous interval for each case (i.e. 2.5 PRF_{avg}). For completeness, a histogram of peak Doppler sidelobe for the entire unambiguous interval is also included for the $K = 50$ case (over 25 PRF_{avg}). Because it covers a 10× greater Doppler span it is not surprising that the latter case (in black) is shifted farthest right. However, while the extent of values shown only covers a few dB, a clear separation is evident for purely random staggering as a result of redundancy when Doppler span is held constant, suggesting a useful trade-space.

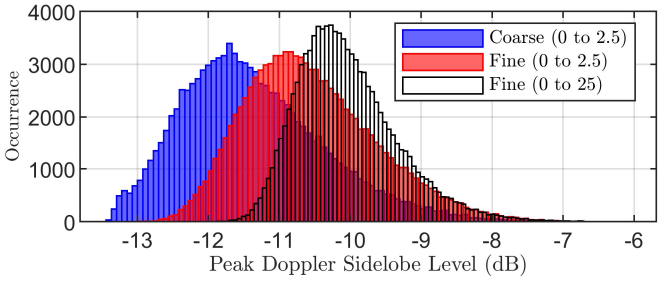

Fig. 8. Histograms of peak Doppler sidelobe for higher redundancy (blue), and lower redundancy (red), and lower redundancy over larger Doppler span (black) for completely random PRI sequences

Further insight can be obtained by examining a single pair of random instantiations for each level of granularity, as shown in Figs. 9 and 10. The co-arrays in Fig. 9 reveal that the 10× difference in granularity roughly corresponds to a similar 10× change in the degree of redundancy, with the caveat that at some point finer granularity would make no further difference.

The Doppler responses in Fig. 10 provide an even more interesting observation when one considers the relationship between the Doppler sidelobe level and the span of unambiguous Doppler for random instantiations. Specifically, the $K = 50$ case extends unambiguous Doppler out to 25 PRF_{avg}, while the $K = 5$ case extends only to 2.5 PRF_{avg}. However, the latter also exhibits lower Doppler sidelobes than the former. Taken together, these imply a trade-space between how flat/low the Doppler sidelobes can be made vs. the degree of

unambiguous Doppler expansion that random staggering can achieve.

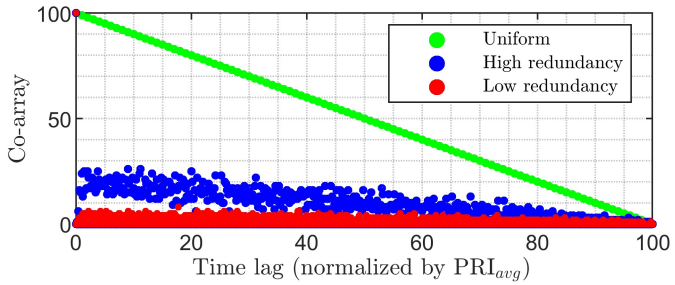

Fig. 9. Co-arrays for uniform, high redundancy, and low redundancy randomized PRI sequences

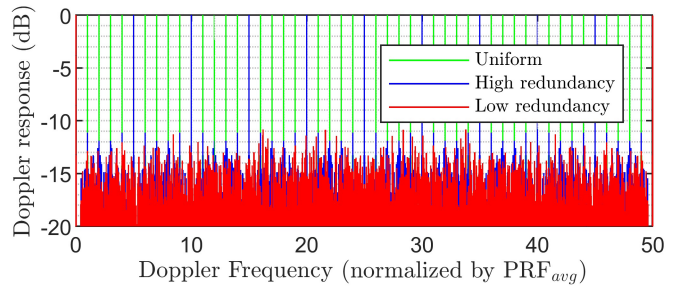

Fig. 10. Doppler response for uniform, high redundancy, and low redundancy randomized PRI sequences

IV. Staggering Co-array Structures

Based on the observation that some degree of redundancy in the staggering co-array may be useful, we consider a couple cases to understand the benefit of particular structures. While linearly staggered PRI structures have been examined for SAR to mitigate blind regions [21-23], here we examine nonlinear structures for the purpose of expanding Doppler. Note that these examples are for illustrative purposes and do not necessarily satisfy practical requirements such as ensuring a minimum allowable PRI.

A. Exponential

A location vector that realizes a co-array having a structure somewhat similar to that in Fig. 9 can also be generated via

$$w_{\exp}(n)=\begin{cases}1, & \text{if } n=\text{rnd}\left\{(m/M)^{\alpha}MK\right\}\\ 0, & \text{otherwise}\end{cases}, \qquad (3)$$

for $n=0, 1, 2, \ldots, MK-1$, pulse index $m=0, 1, \ldots, M-1$, exponential parameter α, and rnd$\{\cdot\}$ indicates rounding to the closest discretized location. Figs. 11-13 depict the behavior of this type of sequence for $M=100$ pulses, $K=5$, and $\alpha=1.391$.

Specifically, Fig. 11 illustrates the exponential stagger structure across the CPI. Clearly the early impulses might be too close together to provide a reasonable listen interval and may not satisfy a minimum PRI requirement. However, the purpose here is to examine the general behavior of the stagger structure on the co-array and Doppler response. We observe in Fig. 12 that the ensuing co-array does produce redundancy that is qualitatively similar to a given random instantiation having the same granularity. Consequently, the extended Doppler response in Fig. 13 likewise exhibits flattened sidelobes over the depicted interval. In fact, the exponential Doppler response is noticeably flatter than that of this particular random case, which exhibits some spurious sidelobes that could potentially cause false alarms. While again noting the practical limitations above, this result suggests a prospective benefit to such nonlinear stagger structures.

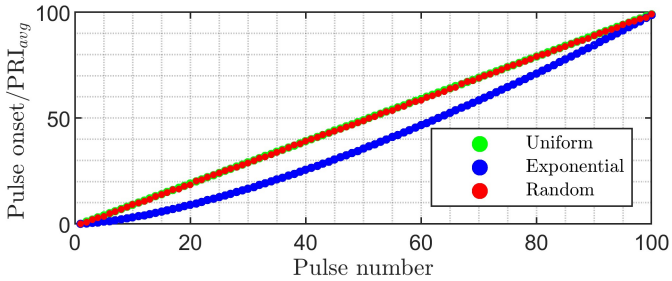

Fig. 11. Pulse onset times for uniform, exponential, and random PRI sequences with 100 pulses

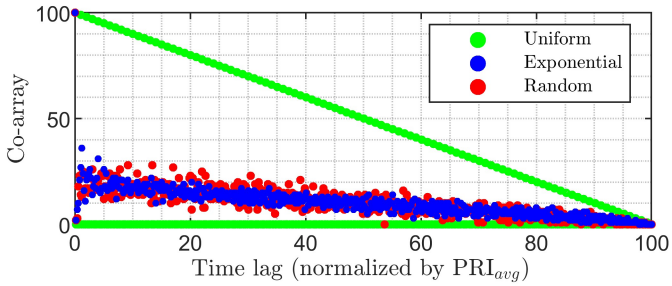

Fig. 12. Co-array for uniform, exponential, and random PRI sequences with 100 pulses

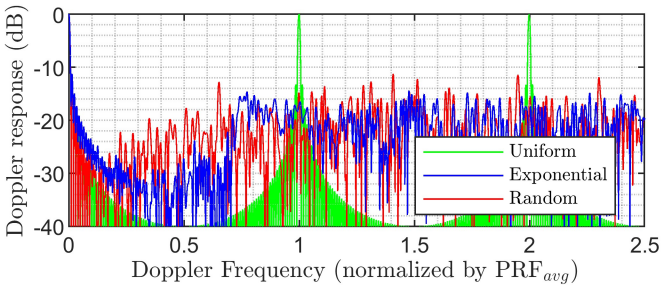

Fig. 13. Doppler response for uniform, exponential, and random PRI sequences with 100 pulses

B. Sine-Exponentiated

The potential benefit of the nonlinear exponential structure suggests others may be useful as well. One in particular that is known to be beneficial for radar waveforms can be generally denoted as a "sideways-S" shape in time/frequency [24], for which there are a number of varieties [2]. For example, consider the sine-exponentiated structure from [25], where an associated location function is

$$w_{\text{se}}(n)=\begin{cases}1, & \text{if } n=\text{rnd}\left\{\dfrac{\sin\left(0.5m\pi/b\right)^{\alpha}}{\sin\left(0.5\pi/b\right)^{\alpha}}MK\right\}\\ 0, & \text{otherwise}\end{cases}. \qquad (4)$$

Figs. 14-16 illustrate this case for $M=100$ pulses, $K=5$, $b=1.1$, and $\alpha=1.253$. Now the stagger structure (Fig. 14) exhibits a "cross-over" around pulse number 20 relative to uniform staggering. The resulting co-array and Doppler

response are similar to the previous case in terms of the degree of observed redundancy and flattened sidelobes, respectively. Again, the takeaway is the prospective benefit of nonlinear stagger structures, now suggesting the time/frequency parameterizations of nonlinear FM waveform designs could provide useful structures to explore.

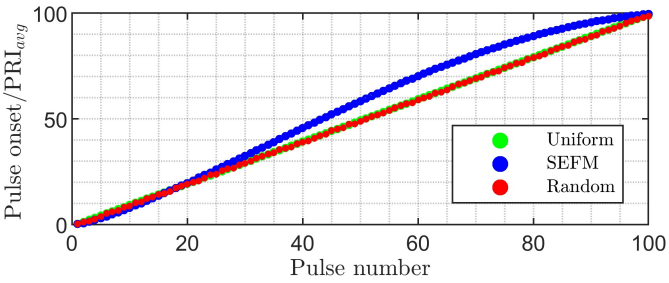

Fig. 14. Pulse onset times for uniform, sine-exponentiated, and random PRI sequences with 100 pulses

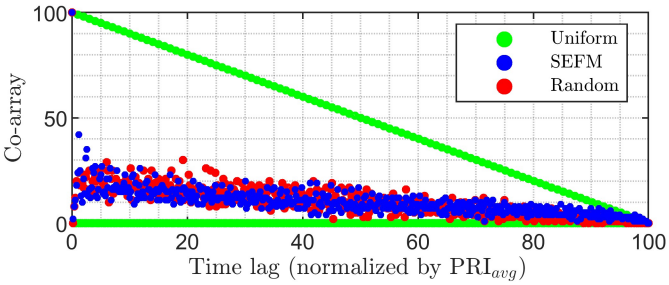

Fig. 15. Co-arrays for uniform, sine-exponentiated, and random PRI sequences with 100 pulses

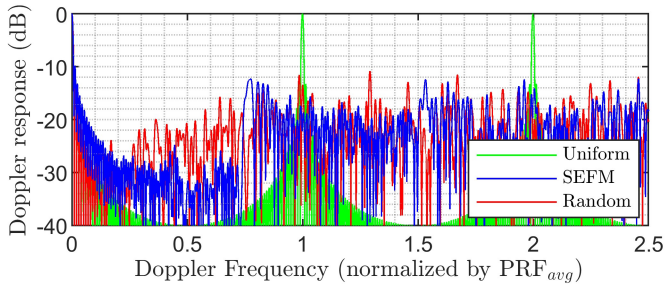

Fig. 16. Doppler response for uniform, sine-exponentiated, and random PRI sequences with 100 pulses

V. Conclusions

Non-uniform sampling underlies both sparse antenna arrays and PRI staggering. Exploiting this analogy and posing staggering as a notional temporal aperture containing pulse "locations" permits exploration of the co-array concept. Interestingly, while minimizing redundancy is known to be a useful goal for sparse array design, it has been found that staggering co-arrays can actually benefit from some redundancy since only a portion of the (essentially) unbounded Doppler span needs to be considered (i.e. there is a meaningful limit on mover velocities). Consequently, a trade-space emerges regarding the meaningful Doppler span and the achievable sidelobe flatness that bears further examination, especially in the context of instantiating random PRI sequences on-the-fly without incurring the computational cost of optimization.

References

[1] M.A. Richards, J.A. Scheer, W.A. Holm, *Principles of Modern Radar: Basic Principles*, SciTech Publishing, 2010.

[2] N. Levanon, E. Mozeson. *Radar Signals*. John Wiley & Sons, Inc., 2004.

[3] D.C. Schleher. *MTI and Pulsed Doppler Radar.* Artech House, Inc., 1991.

[4] M. Kaveh, G.R. Cooper, "Average ambiguity function for a randomly staggered pulse sequence," *IEEE Trans. Aerospace & Electronic Systems*, vol. AES-12, no.3, pp. 410-413, May 1976.

[5] L.B. Milstein, "Reduction of eclipsing loss in high PRF radars," *IEEE Trans. Aerospace & Electronic Systems*, vol. AES-14, no. 2, pp. 410-415, Mar. 1978.

[6] L. Vergara-Dominguez, "Analysis of the digital MTI filter with random PRI," *IEE Proc. F - Radar & Signal Processing*, vol. 140, no. 2, pp. 129-137, Apr. 1993.

[7] Z. Liu, X. Wei, X. Li, "Aliasing-free moving target detection in random pulse repetition interval radar based on compressive sensing," *IEEE Sensors Journal*, vol. 13, no. 7, pp. 2523-2534, July 2013.

[8] J. Zhu, T. Zhao, T. Huang, D. Zhang, "Analysis of random pulse repetition interval radar," *IEEE Radar Conf.*, Philadelphia, PA, May 2016.

[9] X. Long, K. Li, J. Tian, J. Wang, S. Wu, "Ambiguity function analysis of random frequency and PRI agile signals," *IEEE Trans. Aerospace & Electronic Systems*, vol. 57, no. 1, pp. 382-396, Feb. 2021.

[10] S.D. Blunt, L.A. Harnett, B. Ravenscroft, R.J. Chang, C.T. Allen, P.M. McCormick, "Implications of diversified Doppler for random PRI radar," to appear in *IEEE Trans. Aerospace & Electronic Systems*.

[11] J. Ward, "Space-time adaptive processing for airborne radar," MIT Technical Report ESC-TR-94-109, Dec. 1994.

[12] H.L. VanTrees. *Optimum Array Processing: Part IV of Detection, Estimation, and Modulation Theory.* John Wiley & Sons, Inc., 2002.

[13] P.M. McCormick, "Design and optimization of physical waveform-diverse and spatially-diverse radar emissions," University of Kansas, Ph.D. dissertation, May 2018.

[14] P. Anglin. "The application of marginal Fisher's information to radar transmit coding and temporal sampling arrays," University of Kansas, Master's thesis, 2010.

[15] J. Stiles, J. Jenshak, "Sparse array construction using marginal Fisher's information," *Intl. Waveform Diversity & Design Conf.*, Kissimmee, FL, Feb. 2009.

[16] G. Di Martino, A. Iodice, "Coprime synthetic aperture radar (CopSAR): a new acquisition mode for maritime surveillance," in *IEEE Trans. Geoscience & Remote Sensing*, vol. 53, no. 6, pp. 3110-3123, June 2015.

[17] A. Moffet, "Minimum-redundancy linear arrays," *IEEE Trans. Antennas & Propagation*, vol. 16, no. 2, pp. 172-175, Mar. 1968.

[18] A.V. Oppenheim, D. Johnson, K. Steiglitz, "Computation of spectra with unequal resolution using the fast Fourier transform", *Proc. IEEE*, vol. 59, pp. 299-301, Feb., 1971.

[19] L.A. Harnett, B. Ravenscroft, S.D. Blunt, C.T. Allen, "Experimental evaluation of adaptive Doppler estimation for PRI-staggered radar," *IEEE Radar Conf.*, New York, NY, Mar. 2022.

[20] R.J. Chang, C.C. Jones, J.W. Owen, S.D. Blunt, "Gradient-based optimization of random PRI staggering", in preparation for *IEEE Trans. Radar Systems.*

[21] M. Sun, Q. Wei, Y. Yu, Z. Liu and W. Li, "Nonuniform resampling for staggered SAR," *IEEE Intl. Geoscience & Remote Sensing Symp.*, Milan, Italy, July 2015.

[22] M. Villano, G. Krieger, M. Jäger, A. Moreira, "Staggered SAR: performance analysis and experiments with real data," *IEEE Trans. Geoscience & Remote Sensing*, vol. 55, no. 11, pp. 6617-6638, Nov. 2017.

[23] W. Xu, et al., "Continuous PRI variation and phase center adjustment for azimuth uniform sampling in staggered SAR," *IEEE Trans. Geoscience & Remote Sensing*, vol. 60, pp. 1-13, May 2021.

[24] S.D. Blunt, E.L. Mokole, "Overview of radar waveform diversity," *IEEE Aerospace & Electronic Systems Mag.*, vol. 31, no. 11, pp. 2-42, Nov. 2016.

[25] S. Alphonse, G.A. Williamson, "Novel radar signal models using nonlinear frequency modulation," *European Signal Processing Conf.*, Lisbon, Portugal, Sept. 2014.